Supplementary Notes

More than 300 paleomagnetic samples from 6 drill sites were subjected to detailed stepwise demagnetization. All shore based analysis was based on detailed thermal demagnetization (see Kelemen et al., 2004 for a description of shipboard analysis techniques). Prior to the first heating step, most samples were subjected to low temperature (77K) cycling in zero field to preferentially demagnetize larger magnetite grains that may be most susceptible to drilling induced remanence. On average this low temperature treatment removed about 25% of the remanence, with oxide-rich gabbros from Hole 1270B showing the most remanence loss (average 75%).

Figure 5 illustrates representative demagnetization diagrams for Leg 209 samples. Most samples exhibit relatively simple demagnetization behavior, with univectorial decay to the origin after removal of a steep low-stability component related to drilling. The magnitude of the steep drilling-induced component varies considerably, ranging from negligible in many gabbro samples (Fig. 5a) to the dominant component in oxide-rich gabbros (Fig. 5f). Serpentinized peridotites typically have a broad range of unblocking temperatures extending to 580°C (Fig. 5c), consistent with the presence of relatively coarse magnetite.

Gabbroic rocks yielded complex magnetizations, consisting of a drilling induced remanence plus up to three (typically one) components. A high temperature magnetite component, with a narrow range of unblocking temperatures close to 580ºC, was identified in all samples (Figs. 5a,d,e,f). Thermal rather than chemical remanent acquisition best explains the fact that some gabbroic samples carry up to three components with sharp breakpoints with no overlap of their unblocking temperatures (McClelland-Brown, 1982).

Approximately 40% of the gabbro samples exhibit a higher temperature component (representing on average 2% of the NRM) with maximum unblocking temperatures near 680°C (Fig. 5e) that we attribute to hematite. In half these samples the hematite component is approximately colinear (within 10°) with the magnetite direction and can be reasonably interpreted as a product of early high temperature alteration. We interpret the remaining hematite components (including 5 samples where this component is approximately antipodal to the magnetite component, Fig. 5e) as representing late stage oxidative alteration. We therefore use the magnetite component exclusively for estimating the amount of rotation.

Average inclinations and asymmetric 95% confidence bounds were estimated using the inclination only method of McFadden and Reid (1982). A total of 10 samples with only a drilling-related magnetization, defined as a single steep (> 65º) component, were eliminated from the site means. We have calculated separate averages for different lithologies, which may acquire remanence at different times. For Hole 1275D, troctolitic samples the upper 50m exhibit complex magnetizations (Fig. 6) that likely reflect a complex alteration history. Troctolitic samples were excluded from the average inclinations at all sites. Stable remanence directions from alternating field demagnetization of archive half cores (see Kelemen et al., 2004) corroborate the discrete sample results, including the positive inclinations associated with later diabase intrusions.

We also tested whether local incoherent rotations (e.g. from fault zones, breccias) might be recognized using the mesoscopic foliation and remanence directions (Fig. 7). For peridotite sites where a penetrative mesoscopic foliation of constant dip could be identified (such as in site 1274), reorientation of this foliation into a common reference frame using the remanent declination was used to test for structural coherence. We used the anisotropy

of magnetic susceptibility (AMS) as a proxy for the mesoscopic foliation (Lawrence et al., 2002) and used the remanent declination to reorient this fabric to a common reference frame. Samples with reoriented foliations at angles >45º from the average foliation were interpreted to be affected by incoherent rotations (blocks bounded by faults) and were excluded from the statistics. The filtered sample collection has a mean that is ~4° steeper than for the complete data set (Fig. 7), suggesting that incoherent rotations may contribute to the observed shallow inclinations but are unlikely to be the dominant cause of these shallow directions.

Remanence anisotropy is also a possible complicating factor in interpreting inclination data from Leg 209. We determined the anisotropy of thermal remanent magnetizaiton (TRM) for ~100 samples. Each of these samples was given a TRM by cooling from 600°C in six axial directions ($\pm X, \pm Y, \pm Z$) and the resulting anisotropy tensor calculated. Eighty percent of the samples were statistically anisotropic, with an average degree of anisotropy of P=1.20 (where P = ratio of maximum/minimum eigenvalues) and a maximum value of P=1.96. With the exception of three samples, the maximum calculated deviation of the remanent inclination is ±5° and the mean deviation is approximately zero, indicating that remanence deflection is unlikely to impart a systematic bias to the average inclination values.
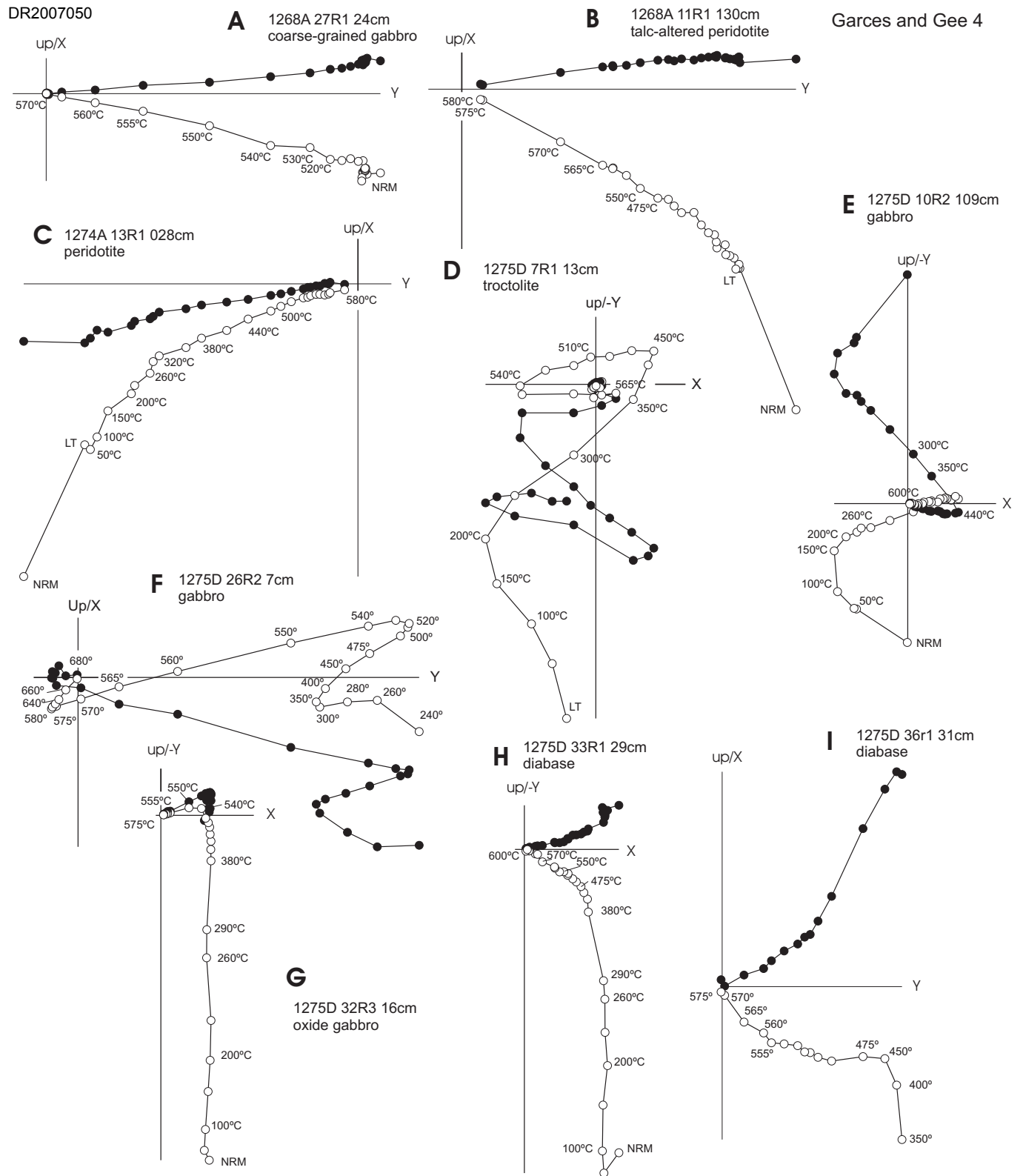
Supplementary Figure 5. Vector endpoint demagnetization diagrams of representative samples. (a) Coarse-grained gabbro illustrating narrow range of high unblocking temperatures. (b) Talc-altered peridotite and (c) serpentinized peridotite samples with nearly univectorial demagnetization behavior. Troctolitic (d) and gabbroic (e, f) samples with multiple remanence components. Note that the hematite component in Fig. 5f has a steeper inclination than the predominant magnetite component, suggesting that late stage oxidative alteration is responsible for the hematite remanence. (g) Oxide-rich gabbro sample illustrating the dominant near vertical drilling induced remanence. (h, i) Diabase samples illustrating moderate positive inclinations. Filled circles are projections onto the horizontal plane and open circles are projections onto the vertical plane. LT denotes remanence after low temperature (77K) treatment.
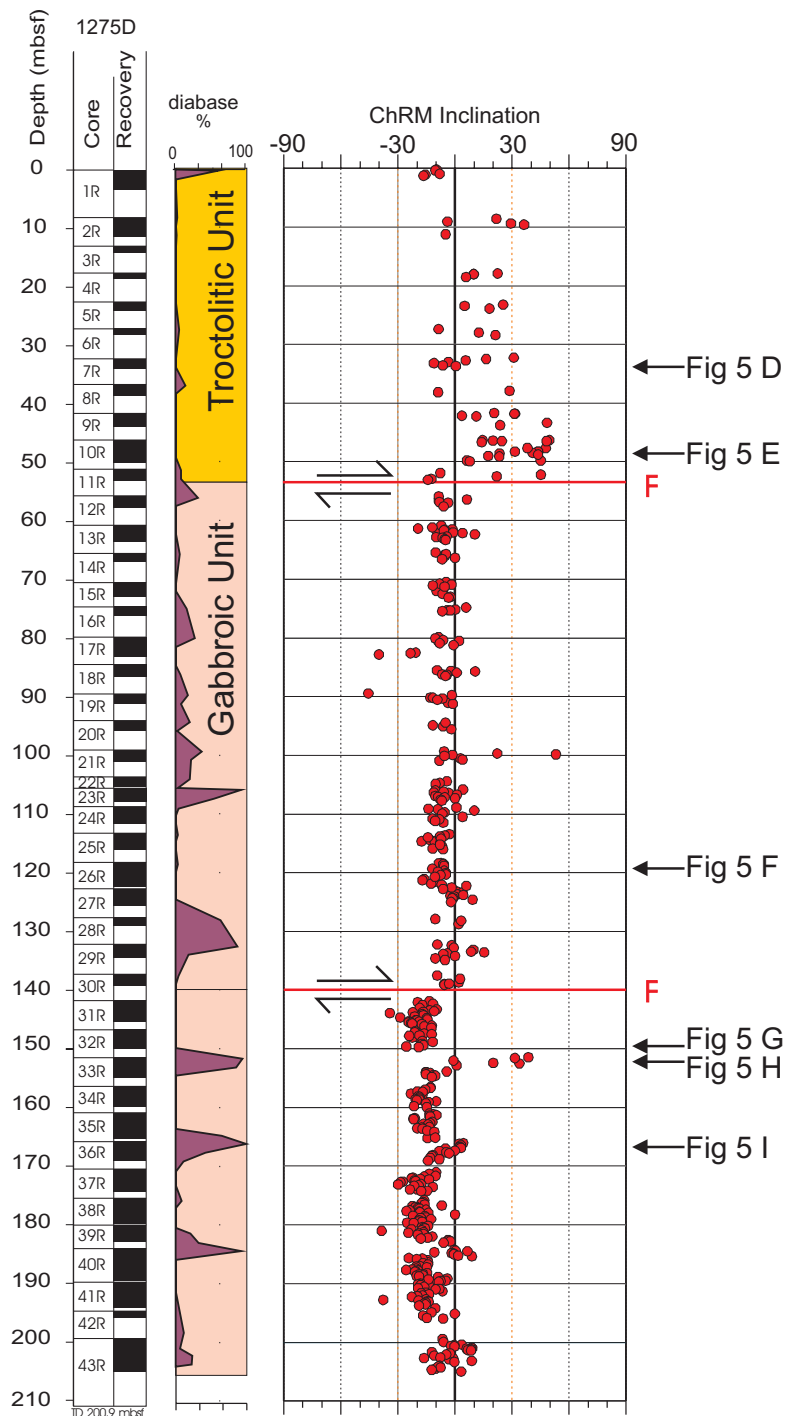
Supplementary Figure 6. Downhole variation in stable inclination of Hole 1275D from archive half core measurements. Each data point represents the principal component calculated from stepwise AF demagnetization (Kelemen et al., 2004). Note the correlation of more positive inclinations with the abundant of finer grained diabase (column at left). F indicates the location of inferred faults. Arrows indicate the location of discrete samples of Fig. 5..
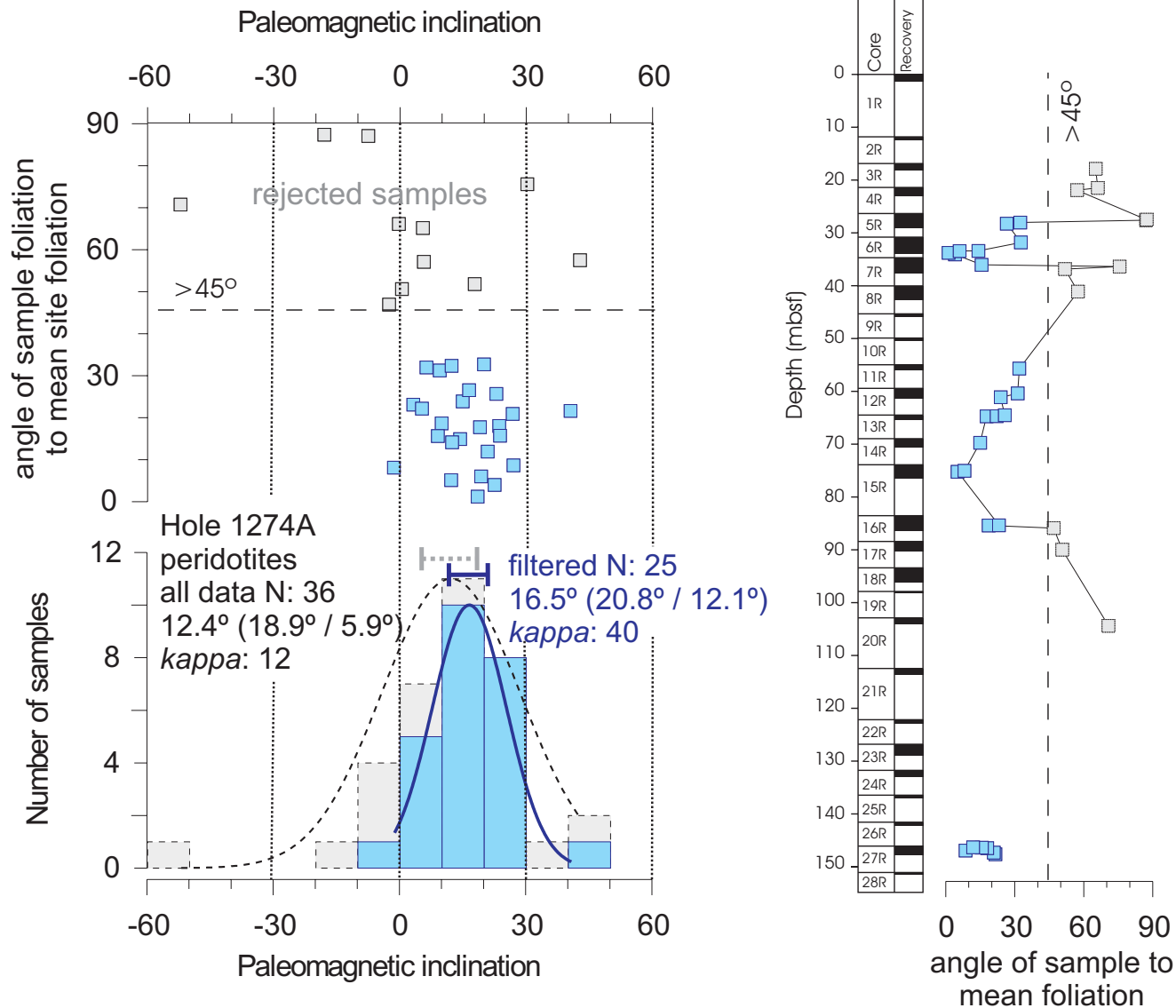
Supplementary Figure 7. Test for structural coherence in serpentinized peridotite samples from Hole 1274A. Left hand diagrams illustrate the deviation of the magnetic foliation (determined from anisotropy of magnetic susceptibility) from the mean foliation after restoration to a common reference frame using the remanent declination. It shows that the samples that deviate more than 45° from the average foliation orientation, also show a large scatter of paleomagnetic inclinations, a fact that suggest that these samples may represent fault bounded blocks affected by independent rotations. Inclination histograms illustrate the effect of removing samples that deviate by more than 45° from the average foliation orientation: increasing kappa values from 12 to 40 indicates that filtering has eliminated a significant portion of incoherent data. Diagram at right illustrates the downhole variation of the angular deviation from the average foliation, and shows that the discrepant samples are clustered in three specific depth intervals corresponding to 17-28, 36-41 and 85-105 mbsf.